Blue-Shifting Hydrogen Bonds

Kersti Hermansson†

Materials Chemistry, The Ångström Laboratory, Uppsala University, Box 538, S-751 21 Uppsala, Sweden

Received: December 4, 2001; In Final Form: February 5, 2002

In this paper we put forward the idea that the various "improper, blue-shifting" hydrogen bond systems discussed in the literature are all of essentially the same nature and occur because of three necessary circumstances: (i) the presence of a negative dipole moment derivative, $d\mu^0/dr_{XH}$, for the isolated H-bond donor molecule; (ii) the interaction between such a molecule and *any* electron density concentration on the H-bond acceptor (π-system density, lone-pair density, ionic charge, ...) which at large intermolecular distances gives rise to a field-dominated, modest vibrational blue shift; (iii) an additional blue shift due to electronic exchange overlap. The negative dipole moment derivative is a necessary but not sufficient condition for the formation of a blue-shifted H-bond: thus, the blue-shifting CH_4, F_3CH, and Cl_3CH molecules and their relatives can also give rise to "normal", red-shifted H-bonds. This is a logical extension of the blue-shifting property and occurs when the electric field from the acceptor is sufficiently strong at the intermolecular equilibrium distance (e.g., for F^- and Cl^- acceptors).

1. Introduction

Some molecules contain intramolecular bonds which are strengthened, shortened, and blue-shifted (upshifted) in stretching vibrational frequency when the molecule is involved in intermolecular bonding. This behavior is relatively unusual. A few examples are CO (see, for example, refs 1−4), CN,[5,6] CN^-,[5] and CH_3CN,[7] where experiment and ab initio calculations have demonstrated that blue shifts occur in different bonding situations or when the molecules are exposed to electric fields ("positive vibrational Stark tuning rate"). Some H-containing molecules display a similar behavior. Blue-shifting hydroxide ions in crystalline hydroxides have been investigated in many IR and Raman spectroscopic studies by the group of Lutz et al. (see for example refs 8 and 9) and by Wickersheim[10] and also by ab initio crystal calculations.[11]

The characteristics of red-shifting and blue-shifting hydrogen bonds are as follows: When a water molecule or a hydrogen halide molecule, for example, approaches an electronegative atom from a favorable, stabilizing direction, a hydrogen bond (X−H···Y) forms and manifests itself in an elongation of the X−H bond, a downshift of the ω(X−H) stretching vibrational frequency, and an IR intensity increase of the stretching vibration. This behavior is true for most polar H-containing molecules bonded to an electronegative neighbor atom in the gaseous, liquid, or solid phases. However, these three features (elongation, red shift, and IR intensity increase) are all reversed in blue-shifting hydrogen bonds, which are nevertheless stabilizing.

In this paper we will mainly be concerned with C−H bonds. Many hydrogen-bonded CH bonds display blue shifts. Caminati et al. noticed a CH frequency upshift in the $F_2HCH\cdots F_2HCH$ system, using both free jet millimeter-wave absorption spectroscopy and ab initio calculations.[12] A CH blue shift of the chloroform molecule has been observed in different solutions with chloroform acting as the solvent.[13−15] Blue shifts of the CH stretching vibration in $Cl_3CH\cdots$benzene and $Cl_3CH\cdots$fluorobenzene gas-phase clusters have been measured by double-resonance infrared ion-depletion spectroscopy.[16] Many of these blue shifts have been confirmed by ab initio calculations performed by the Hobza group for numerous small complexes involving $F_nH_{3-n}CH$ and Cl_3CH molecules.[15] Indirect experimental evidence for a shortening of the donor C−H bond in hydrogen-bonded complexes has also been provided by NMR measurements of $^1J(^{13}C-^1H)$ spin−spin couplings (see, e.g., refs 17 and 18 and a review article concerning the interpretation of these couplings in ref 19).

There is thus today hardly any doubt that bond-length-contracted and vibrationally blue-shifting C−H bonds exist, and their characteristics are by now well-known and have been satisfyingly reproduced by accurate quantum-chemical calculations. However, *the underlying reasons for the frequency blue shift are less clear*. Gu, Kar, and Scheiner[20] performed ab initio calculations for the normal, red-shifting water dimer and the blue-shifting fluoroform···water complex and concluded that there are no fundamental differences in the nature of the bonding in these red-shifting and blue-shifting H-bonded complexes. Cubero et al. made a comparative "Bader analysis"[21] of the total electron density distribution for normal and blue-shifting hydrogen-bonded complexes and found no essential differences between the two classes of complexes.[22] Recently, Masunov, Dannenberg, and Contreras[23] analyzed the r(CH) change and the electron density shift as a function of the external field strength for the C−H bonds in the CH_4, acetylene, and HCN molecules. The methane CH bond contracts, the others elongate, and the authors suggested that the H-bonding behavior of these three molecules can be explained solely on the basis of their different behavior in an electric field.

As mentioned, Hobza et al. have performed high-quality ab initio calculations for numerous blue-shifting complexes between hydrogen-bond donors (such as methane, fluoroform, chloroform, bromoform, and iodoform) and different hydrogen-bond acceptors (such as π-systems (benzene and fluorobenzene), oxygen lone-pair acceptors, and negative ions). These authors have also presented explanations for the CH frequency blue shifts in the different cases. They conclude that in the $Cl_3CH\cdots\pi$ systems, the CH blue shift mainly originates from

† E-mail: kersti@mkem.uu.se.

10.1021/jp0143948 CCC: $22.00
Published on Web 04/17/2002

the *dispersion interaction*,[16,24] while, in the $F_3CH\cdots\pi$ systems, the blue shift originates from a small *charge transfer* from the benzene ring to the fluoroform F atoms.[25] For fluoroform involved in some CH⋯O bonds, such as $F_3CH\cdots OC_2H_4$ (ethylene oxide), Hobza and co-workers suggest that it is the fluoroform molecule's *negative sign of the dipole moment derivative* with respect to the stretching coordinate, $d\mu^0/dr_{CH}$, which is responsible for the blue shift,[26] while in other cases, such as $F_3CH\cdots OH_2$, the *charge transfer* to the F atoms was said to be responsible.[15] When the hydrogen-bond acceptor is an anion, a few different cases are presented: the CH red shift found for methane in $H_3CH\cdots Cl^-$ is explained as a *normal, traditional hydrogen bond*, while the blue-shifting $BrH_2CH\cdots Cl^-$ and $IH_2CH\cdots I^-$ hydrogen bonds are supposedly the result of *charge transfer* from the anion to the halide atom on the opposite side of the C atom.[15]

The purpose of this paper is to show that the situation is not as complicated as has been presented so far in the literature. In this author's opinion, all the cases above (and even the normal red-shifting water dimer!) behave similarly to each other, in the sense that the underlying reasons for the C−H (or O−H) frequency shift are essentially the same in all cases. Moreover, it will be shown that neither the electron charge transfer nor the dispersion interaction is a primary reason behind the blue-shifting CH⋯O or CH⋯π bonds. The reasons for the blue-shifting CH bonds lie in the sign of the dipole moment derivative with respect to the stretching coordinate combined with electronic exchange overlap at moderate and shorter H-bonded distances.

The following hydrogen-bond donors are included in this study: H_2O; CH_4; CHF_3; $CHCl_3$. And the following hydrogen-bond acceptors are discussed: $\cdots\pi$-C_6H_6; $\cdots OH_2$; $\cdots OC_2H_4$; $\cdots Cl^-$. In addition, the frequency shifts for some related "hydrogen-bond donor⋯point-charge acceptor" complexes will be discussed as a means to distinguish between "electrostatic + polarization" effects on one hand and electronic overlap effects on the other.

2. Method

2.1. Quantum-Chemical Calculations. All calculations reported here were performed at the Hartree−Fock level using the cc-pVDZ basis set[27] and the Gaussian 98 program.[28]

In earlier work[29,30] we studied the intramolecular OH frequency shifts of water and hydroxide ions in different environments and compared the results at the Hartree−Fock, MP2, and MP4 levels, using both modest and virtually saturated basis sets. The trends and chemical conclusions at the different levels were the same. In this paper we want to set right a few misconceptions in the literature and discuss the trends in the frequency shifts; we therefore keep the calculations as simple as possible and do not routinely include dispersion (although it is included in the last section of this paper where dispersion effects are discussed). Incidentally, as a check, some of the $\Delta\omega$(CH) vs $F_{||}$ curves in Figure 4 were also calculated at the MP2 level. The curves were very similar to the Hartree−Fock curves and can be obtained from the author on request.

2.2. Point-Charge Complexes. In the following (see Figures 3 and 4) we will compare the frequency shifts for the *all-electron complexes* with the frequency shift for complexes where the acceptor molecule has been replaced by a collection of fractional point charges which mimic the real H-bond acceptor molecule. These "*point-charge acceptor molecules*" were generated in the following way. Using the Gaussian program, first the wave function for each of the optimized isolated H-bond-acceptor molecules ($\cdots OH_2$, $\cdots OC_2H_4$, $\cdots\pi$-C_6H_6, $\cdots Cl^-$) was calculated and then so-called "electrostatic potential-derived" point charges at the nuclear sites were generated. These charges reproduce the electrostatic potential in a grid outside the acceptor molecule, and they also reproduce the acceptor molecule's own dipole moment. Incidentally, small changes of the geometry of the point-charge acceptor (e.g., taking the acceptor geometry from its geometry in the optimized complex instead) have no influence on the results presented here.

2.3. Geometry Optimization and Calculation of Uncoupled C−H Stretching Frequencies. The *geometrical arrangements* of the donor⋯acceptor complexes are shown for the point-charge acceptors in Figure 3, and the all-electron complex geometrical arrangements are the same. For ease of comparison, the 3-fold axis of the CHF_3 molecule, i.e., the CH bond direction, was chosen to coincide with the bisector of the acceptor molecule in the case of $\cdots OH_2$ and $\cdots OC_2H_4$. In the case of the $F_3CH\cdots\pi$-C_6H_6 and $Cl_3CH\cdots\pi$-C_6H_6 complexes, the CH bond was chosen to coincide with the normal of the benzene plane through its ring center. Modest alterations of these hydrogen-bond geometries do not affect any of the conclusions given in this paper. Given the angular restrictions just described, the system geometries were fully optimized at the Hartree−Fock/cc-pVDZ level. The exact optimized geometries can be obtained from the author on request.

Subsequent *normal coordinate analyses* (NCAs) were performed using the Gaussian program. In all cases which contain more hydrogen atoms than the one involved in the X−H⋯Y bond, the others were given the mass of a tritium atom (^{3}H) to ensure that the C−H stretch is uncoupled. In the following, we will always write the molecular formulas with H to denote the hydrogen atoms, regardless of their mass. In all cases, inspection of the NCA output confirmed that the C−H stretching mode consisted of a pure C−H stretch involving only the motion of the C and H atoms around the bond center-of-mass.

Each point in the curves in Figures 3 and 4 originates from a ω(CH) calculation at a fixed R(C⋯acceptor) distance, although it was then actually plotted against electric field strength at the vibrating H atom, using the field value from the wave function calculation for the isolated optimized acceptor. In these ω(CH) calculations, the R(C⋯acceptor) distance was kept frozen in the optimization, and all the other geometrical parameters of the H-bond donor were optimized and subsequent NCAs were performed. Also here it was seen that, in all cases, the C−H stretching mode consisted of a pure C−H stretch involving only the motion of the C and H atoms around the bond center-of-mass. We report harmonic frequencies in this paper.

As a check for both the fully optimized systems and those with R(C⋯acceptor) constrained, the vibrational frequency was in many cases also calculated by a second method. Then the one-dimensional, uncoupled C−H vibrational potential energy curves (energy vs r(CH)) were generated from pointwise energy calculations, 0.01 Å apart in r(CH), keeping the bond center-of-mass fixed. The resulting potential energy curve was fitted to a fifth-order polynomial, and the harmonic frequency was calculated from the second-order force constant. The two different ways of calculating the frequency gave the same results within a few cm^{-1}.

3. Results and Discussion

3.1. Frequency Shifts in Uniform and Nonuniform Electric Fields. Figure 1 shows how the intramolecular CH and OH frequencies vary with electric field strength when isolated H_2O, CH_4, CHF_3, and $CHCl_3$ molecules are exposed to a uniform

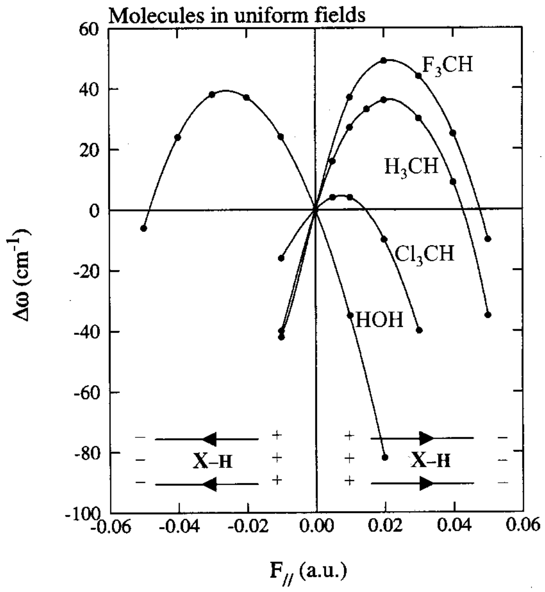

Figure 1. $\Delta\omega$(CH) and $\Delta\omega$(OH) vs the electric field strength along the CH or OH bond for a methane, a chloroform, a fluoroform, and a water molecule exposed to uniform electric fields of various strengths directed along the CH or OH bonds. Here and in the following, $\Delta\omega$ is calculated with respect to the isolated H-bond donor molecule in a field-free environment (i.e., at $F_{||} = 0$ in this figure).

electric field, directed as shown at the bottom of the figure, along the vibrating bond. The positive field direction thus corresponds to the direction with a distant negative charge on the H side of the donor molecule, and this is of course the lower-energy direction compared to the left-hand side of the plot. When the (positive) field is gradually increased, in the range from zero to, for example, 0.01 au, the water OH frequency is seen to redshift while the other three are blue shifted.

Let us review a few basic facts concerning the frequency shift for the intramolecular stretching vibration of a molecule interacting with a *uniform electric field*, $F_{||}$, directed along the vibrating XH bond. The parallel field component is by far the most important in affecting the XH frequency; the perpendicular component has virtually no influence. If $\mu_{||}^0$ is the permanent dipole moment of the isolated molecule in a field-free environment and $\mu_{||}^{ind}$ its induced dipole moment when exposed to the uniform field, then to a good approximation (i.e., neglecting hyperpolarizabilities), the following relation holds for the interaction energy $\Delta E^{ext}(F_{||}, r_{XH})$ of the molecule with the electric field:

$$\Delta E^{ext}(F_{||}, r_{XH}) \approx -F_{||}\cdot[\mu_{||}^0(r_{XH}) + {}^1/_2\,\mu_{||}^{ind}(F_{||}, r_{XH})] \quad (1)$$

In many bonding situations, ΔE is to a good approximation a linear function in r_{XH} (see for example Figure 5), with a slope which we call k^{ext} (for external perturbation), i.e.

$$\Delta E^{ext}(F_{||}, r_{XH}) = k^{ext}(F_{||})\cdot r_{XH} + \text{a constant} \quad (2)$$

Thus, in these cases, to a good approximation, the following relation holds:

$$k^{ext}(F_{||}) \approx -F_{||}\cdot(d\mu^0/dr_{XH} + {}^1/_2\, d\mu^{ind}/dr_{XH}) \quad (3)$$

There is a close correlation between the XH frequency shift and the r(XH) contraction or expansion via the linear perturbation, which gives the following approximate relations:

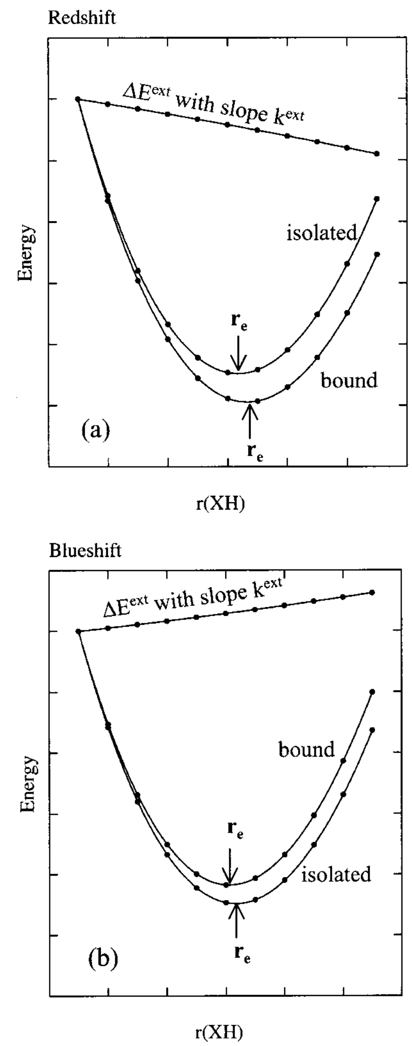

Figure 2. Schematic pictures to explain the signs of the intramolecular bond length shift and the intramolecular stretching frequency shift in the case of a linear external perturbation on the vibrating molecule. ΔE^{ext} is the interaction energy of the molecule with the electric field. All the red-shift cases in Figure 1 can be described by (a), and all the blue-shift situations correspond to (b). The curves have been made to coincide for the shortest r(XH) distance.

$$\Delta r_e \approx -k^{ext} / (2k_2^0) \quad (4)$$

$$\Delta k_2 \approx 3k_3^0\cdot\Delta r_e \quad (5a)$$

$$\approx -3k_3^0\cdot k^{ext} / (2k_2^0) \quad (5b)$$

$$\approx 3k_3^0/(2k_2^0)\cdot F_{||}\cdot(d\mu^0/dr_{XH} + {}^1/_2\, d\mu^{ind}/dr_{XH}) \quad (5c)$$

Here k_2^0 and k_3^0 are the harmonic and cubic force constant for the isolated molecule and Δk_2 is the field-induced shift in k_2, from k_2^0 to its new value at the new r_e. Assuming a negative sign for k_3^0, we thus have

$$\Delta\omega(F_{||}) \propto -F_{||}\cdot(d\mu^0/dr_{XH} + {}^1/_2\, d\mu^{ind}/dr_{XH}) \quad (6)$$

All these relations and their validity were extensively discussed in connection with the red shifts and blue shifts for OH bonds in refs 29−31. To summarize, the interdependence between Δk_2, Δr_e, $d\mu^0/dr_{XH}$, $d\mu^{ind}/dr_{XH}$, and k^{ext} is expressed by the sequence of formulas above, and Figure 2 shows in a schematic way the relations between k^{ext}, Δr_e, and Δk_2 for two different molecules, one with a positive (a) and one with a negative (b) $d\mu^0/dr_{XH}$ value, in fields of modest strengths (so that $d\mu^0/dr_{XH}$ is the dominating dipole moment derivative term).

Expression (6) shows that two basic quantities determine the overall shape of the $\Delta\omega$ vs $F_{\|}$ curve in the case of a linear perturbation, namely the derivative of the molecule's permanent dipole moment with respect to the stretching coordinate, $d\mu^0/dr_{XH}$, and the relative magnitudes of $d\mu^0/dr_{XH}$ and $d\mu^{ind}/dr_{XH}$. The sign of $d\mu^0/dr_{XH}$ determines whether the XH stretching vibration is blue shifted or red shifted when exposed to a field of *small or moderate size*. Since $d\mu^{ind}/dr_{XH}$ is positive (an XH elongation leads to increased induced dipole moment), its action always leads to an overall frequency *red shift at stronger fields*. The net result is an arclike curve (Figure 1).

Four different *nonuniform-field* cases are displayed in Figure 3. In all of these, point charge acceptors mimic the electrostatic properties of a real molecular hydrogen-bond acceptor ($\cdots OH_2$, $\cdots OC_2H_4$, $\cdots\pi$-C_6H_6, $\cdots Cl^-$) as described in the Method part. The different field strengths in the nonuniform field cases were generated by moving the H-bond donor and the point-charge acceptor closer and closer together. The computational procedure to calculate $\Delta\omega$(CH) as a function of a fixed R(C$\cdots$acceptor) distance was also described in the Method section. In the figure, $\Delta\omega$(CH) has been plotted against the electric field strength generated by the point-charge acceptor at the donor H position, when the point-charge acceptor has been placed at different distances away from the CHF_3 molecule.

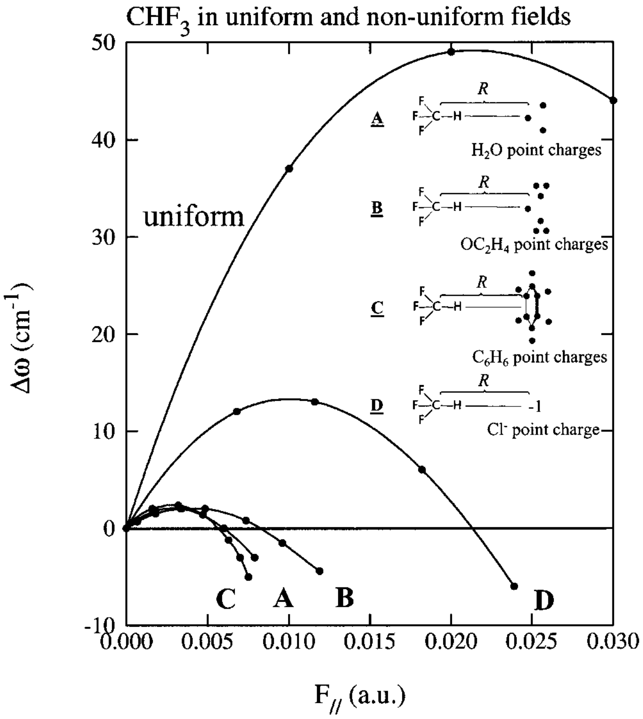

Figure 3. $\Delta\omega$(CH) vs $F_{\|}$ for uniform and nonuniform electric fields exerted on a fluoroform molecule. $F_{\|}$ is the parallel component (along the CH bond) of the electric field strength at the equilibrium position of the H-bonded H atom in each different bonding situation. The "point-charge acceptor complexes" are described in the text.

It is seen from Figure 3 that, in a nonuniform field, the frequency vs field curves differ drastically between each other and from the uniform-field case, but the general form of the curves—with an initial blue shift, a passage over a maximum, and then finally a red shift—is common to all the curves and mainly originates from the negative sign of $d\mu^0/dr_{XH}$ and the overtake from the induced dipole moment term at high electric fields (cf. expression (6)). The large sensitivity to the field nonuniformity is just a demonstration of the fact that the vibrational frequency shift of a molecule in an electric field depends on the electric field at all points in the molecule. The merit of Figure 3 is that it exemplifies and explicitly pinpoints the electrostatic field dependence of the frequency shift for those exact systems that are treated in this paper.

3.2. Total Frequency Shift of Blue-Shifting Molecules. The graphs in Figure 4a–d show the $\Delta\omega$(CH) vs $F_{\|}$ dependence for F_3CH bonded to four different H-bond acceptors and for Cl_3CH H-bonded to benzene. Except for the $F_3CH\cdots Cl^-$ complex in Figure 4d, all *geometry-optimized* complexes (marked with a star in each figure) display CH blue shifts. The water dimer is included for comparison in Figure 4e.

The purpose of each of these curves is to show how the resulting blue shift at the optimized intermolecular distance comes about when the two molecules approach each other from far away. The curves for the corresponding "point-charge acceptor complexes" were shown in Figure 3 and are here repeated for comparison and labeled in the same way as in Figure 3.

Let us first study Figure 4a–c. We note that, in all these cases, the CH group points toward an electron density cloud or some electron density accumulation in the acceptor molecule, and the behavior of the curves is very similar. Thus, at very large donor$\cdots$acceptor distances, there is always a small blue shift. This small blue shift occurs because the very weak external field generated by the acceptor molecule makes the CH bond want to contract, since the contraction increases the permanent F_3CH dipole moment ($\mu_{\|}^0(r_{CH})$) and stabilizes the electrostatic interaction (cf. Figure 2b). The contraction and the blue shift go hand in hand. When the donor and acceptor come sufficiently close, the intermolecular electronic overlap starts to play a vital role, the molecular complexes begin to deviate significantly from the "point-charge acceptor" curves (A–C in Figure 4a–c), and the CH vibration is strongly blue-shifted.

The $F_3CH\cdots Cl^-$ complex (Figure 4d) is consistent with the previous cases. Only here the field from the chloride ion is so strong that the electrostatic effects (including polarization) are allowed to play the major role all the way from large intermolecular distances until where intermolecular electronic overlap sets in, by which time the $\Delta\omega$(CH) vs $F_{\|}$ curve has already passed through its maximum and down on the red-shift side. At the intermolecular equilibrium distance, the overlap has given rise to some additional blue shift but not enough to reverse the sign of the resulting frequency shift, which is indeed a red shift.

The normal hydrogen-bonding water molecule is shown in Figure 4e, where it donates its H atom to another water molecule. For weak external fields, a frequency red shift occurs due to the positive $d\mu^0/dr_{OH}$ value for water. At shorter distances, for example at the dimer intermolecular equilibrium distance, there occurs an additional blue shift due to the electronic overlap, but again, this is not sufficiently strong to reverse the sign of the resulting frequency shift, which is the well-known red shift of the water dimer.

What is the exact origin of the strong blue shift at the optimized intermolecular distances in the case of the fluoroform and chloroform molecules and their relatives? Let us analyze Figure 4a–d in some more detail. Four new contributions to the intermolecular interaction appear when the molecules begin to overlap, namely, the classical electrostatic (Coulombic) + polarization interaction between the now *partially overlapping* molecules, as well as exchange interaction, charge transfer, and

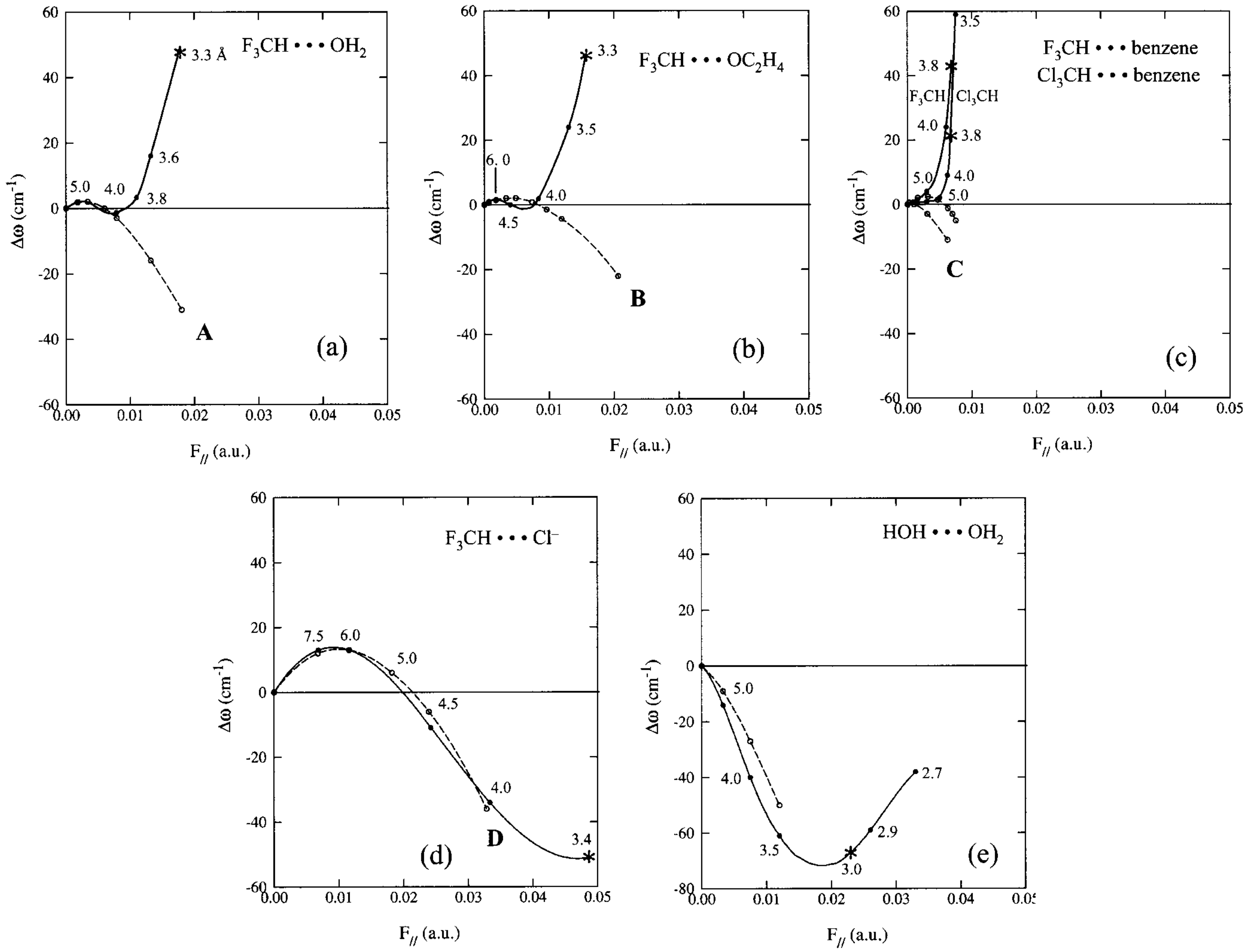

Figure 4. $\Delta\omega$(CH) vs $F_{\parallel}$ for (a) $F_3CH\cdots OH_2$, (b) $F_3CH\cdots OC_2H_4$, (c) $F_3CH\cdots\pi\text{-}C_6H_6$, $Cl_3CH\cdots\pi\text{-}C_6H_6$, (d) $F_3CH\cdots Cl^-$, and (e) $HOH\cdots OH_2$. The solid curves refer to the all-electron complexes, and the dashed curves, to the point-charge acceptor complexes. The latter curves are the same as those in Figure 3 and have been labeled in the same way. The numbers along the curves show the corresponding R(C···acceptor) distance, where R is defined in Figure 3. The fully optimized complexes are indicated by stars.

dispersion interaction. Below, a few comments will be given to try to elucidate the relative importance of these types of intermolecular interaction.

3.3. Contributions to the Blue Shift. Several authors in the literature have emphasized the importance of the repulsive electronic interactions between the vibrating molecule and its surrounding crystal lattice or neighboring substrate surface. Early papers dealing with the OH^- ion in crystalline hydroxides[9,32,33] thus discuss the OH blue shift as due to "repulsion effects" with the crystal lattice, and Pacchioni et al.[3] explain the blue shift for CO on MgO(001) as mainly due to Pauli repulsion and refer to this effect as "the wall-effect". Hermansson, on the other hand, showed that the net OH^- blue shift in some crystalline hydroxides to a large extent originates from the negative sign of $d\mu^0/dr_{OH}$ (combined with the positive sign of $d\mu^{ind}/dr_{OH}$).[11,31] Recently, Damin et al.[4] included higher-order terms in a perturbational field treatment of CO on MgO(001); i.e., they took the field nonuniformity into account and found that the electrostatic effects (without polarization, which they found to be negligible) lead to a larger blue shift than with just a uniform-field approach. Contrary to previous findings, they presented the idea that the exchange-repulsion leads to a red shift instead of a blue shift in this case.

One of the reasons we have calculated the "hydrogen-bond donor···point-charge acceptor" curves in the current study is to avoid some ambiguities of interpretation, since all terms in the electrostatic perturbation theory approach (i.e., $-\Delta E(F) = \mu_z^0\cdot F + {}^1/_2\Theta_{zz}^0\cdot\nabla F + {}^1/_6\Omega_{zzz}^0\cdot\nabla^2 F + {}^1/_{24}\Phi_{zzzz}^0\cdot\nabla^3 F + ... + {}^1/_2 a_{zz}^0\cdot F^2 + ...$) are automatically included in our curves, and moreover, we do not have the problem of assuming only one expansion center for the multipolar series.

Role of Electrostatics and Polarization. Here, let us use the $F_3CH\cdots Cl^-$ complex in Figure 4d as an example. The all-electron curve and the curve pertaining to the *point-charge acceptor complex* (marked D) agree well all the way down to R(C···acceptor) ≈ 4 Å. Curve D originates from both the purely electrostatic (Coulombic) interaction and the polarization interaction between the isolated F_3CH molecule and the nonuniform field from the −1 point charge. This is not exactly the same as the electrostatic + polarization interactions in the *all-electron complex*, because there the interaction involves the interaction of F_3CH with every volume element of the extended, continuous electron density distribution of the Cl^- ion. Nevertheless, for distances down to ∼4 Å, the two curves are seen to be very similar.

At the intermolecular equilibrium distance for the all-electron complex, curve D gives a very strong frequency red shift. This is a strong indication that the electrostatic + polarization contributions at the equilibrium distance in the all-electron complex is also a red shift.

TABLE 1: Morukuma Interaction Energy Analysis for the $F_3CH\cdots OH_2$, $F_3CH\cdots Cl^-$, and $HOH\cdots OH_2$ Complexes at Different Hydrogen-Bond Distances[a]

system	R(C···Y) (Å)	r(CH) (Å)	ES	PL	ES + PL	CT	EX	MIX	tot.
$F_3CH\cdots OH_2$	6.0	1.070	−0.525	−0.008	−0.533	0.000	0.000	0.000	−0.533
		1.090	−0.522	−0.008	−0.530	0.000	0.000	0.000	−0.530
		diff	**+0.003**	**0.000**	**+0.003**	**0.000**	**0.000**	**0.000**	**+0.003**
	5.0	1.070	−0.930	−0.024	−0.954	−0.075	+0.001	0.000	−1.029
		1.090	−0.927	−0.025	−0.951	−0.078	+0.001	0.000	−1.028
		diff	**+0.003**	**−0.001**	**+0.003**	**−0.003**	**0.000**	**0.000**	**+0.001**
	4.0	1.070	−1.903	−0.101	−2.004	−0.640	+0.110	0.000	−2.531
		1.090	−1.904	−0.105	−2.009	−0.648	+0.122	0.000	−2.529
		diff	**−0.001**	**−0.004**	**−0.005**	**−0.008**	**+0.012**	**0.000**	**+0.002**
	3.3 (≈R_{eq})	1.070	−4.367	−0.372	−4.739	−1.334	+2.430	−0.030	−3.673
		1.090	−4.462	−0.386	−4.848	−1.385	+2.647	−0.030	−3.616
		diff	**−0.095**	**−0.014**	**−0.109**	**−0.051**	**+0.217**	**0.000**	**+0.057**
$F_3CH\cdots Cl^-$	6.0	1.070	−4.015	−0.296	−4.311	−0.047	+0.001	+0.001	−4.359
		1.090	−3.987	−0.306	−4.293	−0.048	+0.001	+0.001	−4.342
		diff	**+0.028**	**−0.010**	**+0.018**	**−0.001**	**0.000**	**0.000**	**+0.017**
	4.5	1.070	−7.804	−1.035	−8.839	−0.857	+0.184	−0.044	−9.556
		1.090	−7.774	−1.074	−8.848	−0.873	+0.198	−0.045	−9.568
		diff	**+0.030**	**−0.039**	**−0.009**	**−0.016**	**+0.014**	**−0.001**	**−0.012**
	3.5 (≈R_{eq})	1.070	−16.100	−2.930	−19.030	−2.263	+6.311	+0.067	−14.915
		1.090	−16.246	−3.035	−19.281	−2.435	+6.694	+0.073	−14.949
		diff	**−0.146**	**−0.105**	**−0.251**	**−0.172**	**+0.383**	**+0.006**	**−0.034**
$HOH\cdots OH_2$	6.0	0.940	−0.407	0.000	−0.407	0.000	0.000	0.000	−0.407
		0.960	−0.414	0.000	−0.414	0.000	0.000	0.000	−0.414
		diff	**−0.007**	**0.000**	**−0.007**	**0.000**	**0.000**	**0.000**	**−0.007**
	4.0	0.940	−1.820	−0.064	−1.884	−0.673	+0.050	0.000	−2.507
		0.960	−1.872	−0.068	−1.940	−0.688	+0.056	0.000	−2.572
		diff	**−0.052**	**−0.004**	**−0.056**	**−0.015**	**+0.006**	**0.000**	**−0.065**
	2.9 (≈R_{eq})	0.940	−7.544	−0.757	−8.301	−2.114	+5.401	−0.095	−5.109
		0.960	−7.914	−0.822	−8.736	−2.253	+5.859	−0.086	−5.216
		diff	**−0.370**	**−0.065**	**−0.435**	**−0.139**	**+0.458**	**+0.009**	**−0.107**

[a] The total interaction energy ΔE ($=E^{complex} - E^{momoner1} - E^{momomer2}$, with both monomers at the same geometries as in the complex) is partitioned into the following contributions: ES = electrostatic interaction energy; PL = polarization; EX = exchange; CT = electron charge transfer; MIX = remainder terms. ES is the classical Coulombic interaction between the electron density distributions of the unperturbed donor and acceptor species, positioned at exactly the same positions as in the H-bonded complex, and PL is the energy gain caused by the polarization of the electron density of molecule 1 in the field from molecule 2 and vice versa. The energies were calculated using the GAMESS program[35] and are given in kcal/mol. The "diff" rows give the various contributions to k^{ext} (cf. Figure 2).

This indication is further supported by the so-called Morokuma analysis scheme for the decomposition of intermolecular energies[34] (see further description of the method in the caption of Table 1). The results of the Morokuma analysis for the $F_3CH\cdots Cl^-$, $F_3CH\cdots OH_2$, and $HOH\cdots OH_2$ complexes are compiled in Table 1. For each system, three or four intermolecular distances have been investigated, and for each intermolecular distance, *two intramolecular* XH distances. In this way we can calculate the *changes* in the various interaction energy contributions when the donor XH bond is stretched, and this will show the relative importance of the different interaction contributions to k^{ext} (cf. Figure 2) and thus to the total $\Delta\omega$ (using now eq 5b and the general expression $\Delta E^{ext} = k^{ext}\cdot r_{XH}$ + a constant). We find that the Morokuma "ES + PL" energy (third energy column in the table) gives a *negative contribution* to k^{ext} (see "diff" row) at the intermolecular eqilibrium distance for $F_3CH\cdots Cl^-$, in agreement with our conclusion above.

Gu et al.[20] performed a similar kind of Morokuma analysis for the $F_3CH\cdots OH_2$ and $HOH\cdots OH_2$ complexes at their respective intermolecular equilibrium distances and concluded that not only are the ES + PL contributions similar in sign (both negative) in the two complexes but all the energy contributions have the same sign in the two complexes. We obtain the same results in Table 1; cf. the "diff" rows in the two R_{eq} sections for $F_3CH\cdots OH_2$ and $HOH\cdots OH_2$. However, we have also included some weaker-field cases in our discussion of the Morokuma analysis, and now we do detect differences between the blue-shifting and red-shifting molecules! The ES + PL contributions for the $F_3CH\cdots OH_2$ and $F_3CH\cdots Cl^-$ complexes have *postive signs* at large R(X···Y) distances and *negative signs* at R_{eq}(X···Y). The water dimer, on the other hand, has a *negative sign* for all intermolecular distances. We note that the variations of the Morokuma ES + PL contributions follow the point-charge acceptor curves in Figure 4 and they are qualitatively different for the red-shifting and blue-shifting donor molecules.

Role of Charge Transfer. Hobza et al. have argued that, for example in the case of the blue-shifting $F_3CH\cdots OH_2$ complex, a small electron charge transfer to the F lone-pair orbitals (as measured by the natural-bond orbital (NBO) occupancies[36]) leads to a structural reorganization of the fluoroform molecule (an opening of the H−C−F angles and a small elongation of the C−F bonds), which then gives rise to a contraction of the CH bond and a corresponding blue shift of the CH stretching frequency. Here we will try to establish whether such a correlation exists.

Table 2 gives some results from an NBO population analysis for the optimized $F_3CH\cdots OH_2$ complex and for five other cases as well: one blue-shifting and four red-shifting. The magnitudes of the frequency shifts are seen in Figure 4. Table 2 shows that there is nothing unique about the magnitude of the charge transfer or the geometry change in the case of the blue shifting $F_3CH\cdots OH_2$. For example, in a uniform electric field or with

TABLE 2: Changes in Geometry and Orbital Occupancies (NBO Analysis) for Fluoroform in Different Bonding Situations, Compared to the Free Molecule[a]

system	ΔHCF angle (deg)	Δr(CF) (Å)	$\Delta\omega$	Δ(lone-pair occ on F)	cht
charge-transfer impossible					
F_3CH in uniform field ($F_{\|} = 0.02$)	+1.4	+0.01	blue shift	0.01	
F_3CH in uniform field ($F_{\|} = 0.05$)	+3.5	+0.02	red shift	0.04	
$F_3CH\cdots$pt ch OH_2	+0.4	+0.00	red shift	0.01	
$F_3CH\cdots$pt ch Cl^-	+1.3	+0.01	red shift	0.02	
charge-transfer possible					
$F_3CH\cdots OH_2$	+0.5	+0.00	blue shift	0.01	0.005
$F_3CH\cdots Cl^-$	+1.6	+0.01	red shift	0.03	0.023

[a] "Δ(lone-pair occ)" means the change in occupancies summed over all three F atoms (a positive value means a gain of electrons). The last column indicates the amount of electron transfer, where a positive value means a net electron flow from the H-bond acceptor to the fluoroform molecule. All systems were optimized, except the $CHF_3\cdots$point-charges systems, where the "intermolecular distance" was taken to be that of the corresponding water or chloride complex. The free CHF_3 molecule has an H−C−F angle of 110.48° and an r(CF) distance of 1.32 Å, and the sum of the F lone pair occupancies is 17.73 e.

a point-charge acceptor, obviously no charge transfer to the CHF_3 molecule is allowed, yet Table 2 shows that a blue shift can occur also in such cases (of course we knew this already from Figure 3!). Moreover, as far as the increase in lone-pair occupancy on the F atoms is concerned, we find that such an increase can occur regardless of charge transfer, i.e., just due to the polarization from the environment, and moreover, it is found in both red-shifting and blue-shifting H-bonding situations.

We conclude that neither the electron charge transfer to the F atoms nor the small geometrical changes of the $-CF_3$ group appears to play a major role in the blue-shifting phenomenon for F_3CH.

This conclusion is also supported by the Morokuma analysis in Table 1, which contains information about the charge-transfer contribution to the interaction energies and thus to the k^{ext} slope. We note that the charge-transfer contribution to the frequency shift is always a *red shift* according to the Morokuma analysis. This is true for all the charge-transfer entries in the table.

Incidentally, the charge transfer explains why some blue-shifting molecules in very weak-field cases are almost not blue-shifted at all (Figure 4a−c). This happens because the red-shifting charge-transfer contribution sets in already at quite large intermolecular distances, earlier than exchange or dispersion begin to play a role.

Role of Dispersion. It was suggested in the literature[16,24] that the CH blue shift for $Cl_3CH\cdots\pi\text{-}C_6H_6$ is due to electron correlation (dispersion) effects, while the blue shift for the corresponding F_3CH complex is due to charge transfer, as discussed (and rejected) in the previous section. We have seen that for the optimized all-electron complexes in Figure 4a−c a blue shift was always found, without dispersion taken into account. It is thus unlikely that it would play a major role in the blue shifts observed experimentally.

Nevertheless, to cast further light on this issue, we have explicitly calculated the dispersion influence on the frequency shift for $Cl_3CH\cdots\pi\text{-}C_6H_6$. Figure 5 shows ΔE vs r(CH) curves for $Cl_3CH\cdots\pi\text{-}C_6H_6$ at the Hartree−Fock/cc-pVDZ and MP2/cc-pVDZ levels for two different intermolecular distances (in fact, for the intermolecular equilibrium distances at the two computational levels). We note that the Hartree−Fock and MP2 slopes (k^{ext}) are quite similar. Furthermore, we note that dispersion gives rise to a *red shift*. We conclude that dispersion is not responsible for the blue shift.

Role of Exchange. Above we have presented various arguments to show that electrostatic, polarization, charge-transfer, and dispersion effects are not responsible for the blue shift. We will thus have to conclude that among the different interactions which set in when the electron density clouds of the donor and

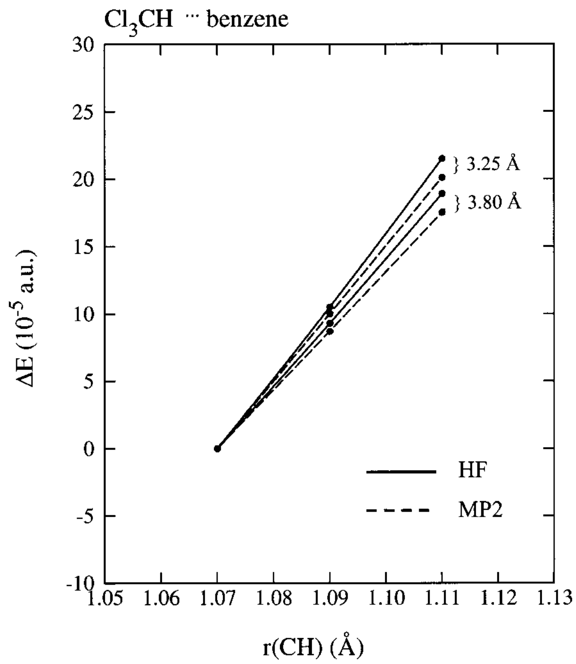

Figure 5. $\Delta E(r_{CH})$ vs r_{CH} for $Cl_3CH\cdots\pi\text{-}C_6H_6$ at the Hartree−Fock/cc-pVDZ and MP2/cc-pVDZ levels for two different $R(C\cdots$benzene) distances, 3.80 and 3.25 Å (the respective optimized distances at these computational levels). The curves have been made to coincide for r(CH) = 1.070 Å to help in the comparison of the slopes.

acceptor molecules begin to overlap, it is the exchange interaction which gives rise to the frequency blue shift at the intermolecular equilibrium distance.

The Morokuma analysis in Table 1 agrees with this conclusion. Indeed, only two of the contributions in the Morokuma analysis give rise to a blue shift, namely the exchange and "Mix" contributions, where exchange is by far the overwhelming part. This is thus the major reason for the blue shift.

However, the negative dipole moment derivative with respect to the stretching coordinate also plays a role, both at long and short intermolecular distances. *At large intermolecular distances* it is the only reason for the blue shift. But also *at shorter distances*, e.g., at the equilibrium distance, it plays a role, because it has by then already helped to "lift the frequency" above what it would be for a donor molecule with a positive dipole moment derivative (such as water), and together with the additional exchange-induced blue shift, the result is a *net blue shift*. This is contrary to the water dimer, where the large exchange-induced blue shift contribution at equilibrium still does not manage to counteract the red-shift contribution from the "electrostatic + polarization" interaction, and the net shift at equilibrium is a red shift (Figure 4e).

4. Conclusions

The purpose of this paper is to convey some insight on the nature of blue-shifting hydrogen bonds. On the basis of our own calculations and the results existing in the literature, we want to draw the following conclusions:

(i) The various cases of blue-shifting CH hydrogen bonds discussed in the literature, namely C−H···π, C−H···O, and C−H···X^- should not be discussed as separate and disparate cases but rather as different manifestations of one and the same phenomenon.

(ii) At *large intermolecular distances* between the H-bond donor and acceptor, the H-bond donor's negative dipole moment derivative with respect to the stretching coordinate is the only reason for the blue shift.

(iii) At the *intermolecular equilibrium distance*, a blue-shifted H-bond appears if the H-bond donor molecule possesses a negative $d\mu^0/dr_{XH}$ value, which is interacting with the electric field from the acceptor molecule, *and at the same time* the exchange interaction between the two molecules is appreciable. The blue-shifting property manifests itself in all chemical systems where the donor molecule interacts with some electron density excess region in the H-bond acceptor (π-system density, anion, lone-pair density, ...)—except for the cases discussed in point iv below.

At the intermolecular equilibrium distance, the largest contribution to the blue shift is from the exchange overlap; nevertheless, the blue shift is made possible by the "groundwork" performed by the arc-shaped electric-field curve, which ensures that when the blue-shifting exchange sets in, the field-induced shift is not already appreciably red-shifted as in the case of the water dimer (and other H-bond donors with positive $d\mu^0/dr_{XH}$ values). Both the electric-field interactions and the exchange overlap are thus responsible for the blue shift in a rather intricate and combined fashion, which was summarized in the section just before the Conclusions. A comparison of Figure 4a ($F_3CH···OH_2$) with Figure 4e (HOH···OH_2) pinpoints the differences beween a blue-shifting and a red-shifting H-bond donor (remember that the stars indicate the equilibrium intermolecular distances).

(iv) A molecule with "the capability of forming blue-shifting H-bonds" displays normal, red-shifting hydrogen bonds when the electric field from the acceptor is strong enough to dominate over the overlap effects at the equilibrium intermolecular distance (example, $F_3CH···Cl^-$ in Figure 4d).

(v) The *small charge transfer to the F atoms* in $F_3CH···OH_2$ is only of minor importance for the frequency shift and leads to a red shift.

(vi) The *dispersion interaction* always gives rise to a red-shift contribution at the intermolecular equlibrium distance.

(vii) Blue-shifting H-bonding molecules form a subclass of all those molecules whose dipole moment increase on intramolecular bond contraction: they all display frequency blue shifts when bound through the partially positive end toward a region with a relatively high electron density.

Acknowledgment. The author thanks the Swedish Research Council (VR) which supported this project financially. Valuable discussions with Dr. Ljupco Pejov (Skopje) are gratefully acknowledged.

References and Notes

(1) Lambert, D. K. *Solid State Commun.* **1984**, *51*, 297.
(2) Bauschlicher, C. W., Jr. *Chem. Phys. Lett.* **1985**, *118*, 307.
(3) Pacchioni, G.; Cogliandro, G.; Bagus, P. S. *Int. J. Quantum Chem.* **1992**, *42*, 1115.
(4) Damin, A.; Dovesi, R.; Zecchina, A.; Ugliengo, P. *Surf. Sci.* **2001**, *479*, 255.
(5) Bauschlicher, C. W., Jr. *Int. J. Quantum Chem.* **1997**, *61*, 859.
(6) Bagus, P. S.; Nelin, C. J.; Müller, W.; Philpott, M. R.; Seki, H. *Phys. Rev. Lett.* **1987**, *58*, 559.
(7) Bertrán, J. F.; Ruíz, E. R. *Spectrochim. Acta* **1993**, *49A*, 43.
(8) Lutz, H. D.; Eckers, W.; Schneider, G.; Haeuseler, H. *Spectrochim. Acta* **1981**, *37A*, 561.
(9) Lutz, H. D.; Eckers, W.; Haeuseler, H. *J. Mol. Struct.* **1982**, *80*, 221.
(10) Wickersheim, K. A. *J. Chem. Phys.* **1959**, *31*, 863.
(11) Hermansson, K.; *Chem. Phys.* **1992**, *159*, 67.
(12) Caminati, W.; Melandri, S.; Moreschini, P.; Favero, P. G. *Angew. Chem., Int. Ed. Engl.* **1999**, *38*, 2924.
(13) Budesinsky, M.; Fiedler, P.; Arnold, Z. *Synthesis* **1989**, 868.
(14) Boldeskul, I. E.; Tsymbal, I. F.; Ryltsev, E. V.; Latajka, Z.; Barnes, A. J. *J. Mol. Struct.* **1997**, *436*, 167.
(15) Hobza, P.; Havlas, Z. *Chem. Rev.* **2000**, *100*, 4253.
(16) Hobza, P.; Spirko, V.; Havlas, Z.; Buchhold, K.; Reimann, B.; Barth, H.-D.; Brutschy, B.; *Chem. Phys. Lett.* **1999**, *299*, 180.
(17) Satonaka, H.; Abe, K.; Hirota, M. *Bull. Chem. Soc. Jpn.* **1987**, *60*, 953.
(18) Alfonin, A. V.; Andriyankov, M. A. *Zh. Org. Khim.* **1988**, *24*, 1034.
(19) Contreras, R. H.; J. E., *Prog. Nucl. Magn. Spectrosc.* **2000**, *34*, 321.
(20) Gu, Y. Kar, T.; Scheiner, S. *J. Am. Chem. Soc.* **1999**, *121*, 9411.
(21) Bader, R. W. F. *Atoms in Molecules. A Quantum Theory*; Oxford University Press: Oxford, U.K., 1990.
(22) Cubero, E.; Orozco, M.; Hobza, P.; Luque, F. J. *J. Phys. Chem. A* **1999**, *103*, 6394.
(23) Masunov, Dannenberg, J. J.; Contreras, R. *J. Phys. Chem. A* **2001**, *105*, 4737.
(24) Hobza, P.; Spirko, V.; Selzle, H. L.; Schlag, E. W. *J. Phys. Chem.* **1998**, *102*, 2501.
(25) Reimann, B.; Buchfold, K.; Vaupel, S.; Brutschy, B.; Havlas, Z.; Spirko, V.; Hobza, P. *J. Phys. Chem. A* **2001**, *105*, 5560.
(26) Hobza, P.; Havlas, Z. *Chem. Phys. Lett.* **1999**, *303*, 447.
(27) Woon, A. E.; Dunning, T. H., Jr. *J. Chem. Phys.* **1993**, *98*, 11358.
(28) Frisch, M. J.; Trucks, G. W.; Schlegel, H. B.; Scuseria, G. E.; Robb, M. A.; Cheeseman, J. R.; Zakrzewski, V. G.; Montgomery, J. A.; Stratmann, R. E.; Burant, J. C.; Dapprich, S.; Millam, J. M.; Daniels, A. D.; Kudin, K. N.; Strain, M. C.; Farkas, O.; Tomasi, J.; Barone, V.; Cossi, M.; Cammi, R.; Mennucci, B.; Pomelli, C.; Adamo, C.; Clifford, S.; Ochterski, J.; Petersson, G. A.; Ayala, P. Y.; Cui, Q.; Morokuma, K.; Malick, D. K.; Rabuck, A. D.; Raghavachari, K.; Foresman, J. B.; Cioslowski, J.; Ortiz, J. V.; Stefanov, B. B.; Liu, G.; Liashenko, A.; Piskorz, P.; Komaromi, I.; Gomperts, R.; Martin, R. L.; Fox, D. J.; Keith, T.; Al-Laham, M. A.; Peng, C. Y.; Nanayakkara, A.; Gonzalez, C.; Challacombe, M.; Gill, P. M. W.; Johnson, B. G.; Chen, W.; Wong, M. W.; Andres, J. L.; Head-Gordon, M.; Replogle, E. S.; Pople, J. A. *Gaussian 98 (Revision A.1)*; Gaussian, Inc.: Pittsburgh, PA, 1998.
(29) Hermansson, K. *J. Chem. Phys.* **1991**, *95*, 3578.
(30) Hermansson, K.; *J. Chem. Phys.* **1993**, *99*, 861.
(31) Hermansson, K. *Int. J. Quantum Chem.* **1993**, *45*, 747.
(32) Bates, J. B.; Quist, A. S. *Spectrochim. Acta* **1975**, *31A*, 1317.
(33) Lutz, H. D.; Henning, J.; Haeuseler, H. *J. Mol. Struct.* **1987**, *156*, 143.
(34) Morokuma, K.; Kitaura, K. In *Molecular Interactions*; Ratajczak, H., Orville-Thomas, W. J., Eds.; Wiley: New York, 1980; Chapter 2.
(35) Schmidt, M. W. Baldridge, K. K.; Boatz, J. A.; Elbert, S. T.; Gordon, M. S.; Jensen, J. H.; Koseki, S.; Matsunaga, N.; Nguyen, K. A.; Su, S.; Windus, T. L.; Dupuis, M.; Montgomery, J. A. *J. Comput. Chem.* **1993**, *14*, 1347.
(36) Glendening, E. D.; Reed, A. E.; Carpenter, J. E.; Weinhold, F. NBO version 3.1, as programmed in Gaussian 98.